

# Pace Time Modulation for Intra-Cardiac Communication

Farrokh Hejri<sup>1</sup>, Mladen Veletić<sup>2</sup>, Ilanko Balasingham, *Senior Member, IEEE*,  
and Peter A. Hoehner<sup>3</sup>, *Fellow, IEEE*

**Abstract**—Although single-node leadless pacemakers eliminate several complications associated with subcutaneous pockets and leads, they have the significant limitation of only being able to perform single-chamber pacing. Multi-nodal pacing can outperform single-chamber pacing by providing a closer approximation of sinus rhythm but requires energy-efficient wireless communication to preserve synchrony. In this work, we propose a novel biocompatible communication concept wherein the pacemaker node located in the sinoatrial (SA) node stimulates the right atrium and simultaneously sends a synchronization message, encoded into the pacing time, to all other pacemaker nodes located at different sites in the heart. We refer to this concept as the Pace Time Modulation (PTM) method and assess its performance in terms of symbol error rate and achievable information rate. The analyses and numerical simulations indicate that PTM can be applicable in realistic scenarios, without deviating the heart rate from its normal range.

**Index Terms**—Biomedical communication, pulse modulation.

## I. INTRODUCTION

**I**NTRA-BODY communications (IBC) technology promises new solutions for several biomedical applications [1]. IBC manifests through electromagnetic communication (EC) and molecular communication (MC). EC in the body considers capacitive-, galvanic-, and inductive-coupling, as well as ultrasound and fat-IBC methods [2], [3]. Such methods are practically difficult to implement due to limitations in power consumption, antenna size, wavelength, and often detrimental radiation. Conversely, MC has better adaptability to biological structures [4], but, due to the slow nature of information carrier advection and diffusion, is limited to applications that can tolerate high communication delays and low data rates, such as disease diagnosis and targeted drug delivery.

Regarding heart applications, adequate IBC is essential for the development of multi-nodal pacemakers. During the past decade, studies have also been conducted exploring different pacing modalities, for example, His Bundle pacing, biventricular pacing, and dual-chamber pacing [5], as well as using pacing algorithms that rely on data acquired from hemodynamic sensors to perform efficient rate-responsive pacing [6].

Manuscript received 19 May 2022; revised 4 July 2022; accepted 21 July 2022. Date of publication 27 July 2022; date of current version 10 October 2022. This work is supported by the Research Council of Norway through the Wireless In-body Sensor and Actuator Networks (WINNOW) Project under Grant 270957. The associate editor coordinating the review of this letter and approving it for publication was M. Egan. (*Corresponding author: Farrokh Hejri.*)

Farrokh Hejri and Ilanko Balasingham are with the Department of Electronic Systems, Norwegian University of Science and Technology (NTNU), 7491 Trondheim, Norway (e-mail: farrokh.hejri@ntnu.no).

Mladen Veletić is with the Intervention Center, Oslo University Hospital, 0424 Oslo, Norway.

Peter A. Hoehner is with the Department of Electrical and Information Engineering, Kiel University (CAU), 24143 Kiel, Germany.

Digital Object Identifier 10.1109/LCOMM.2022.3194268

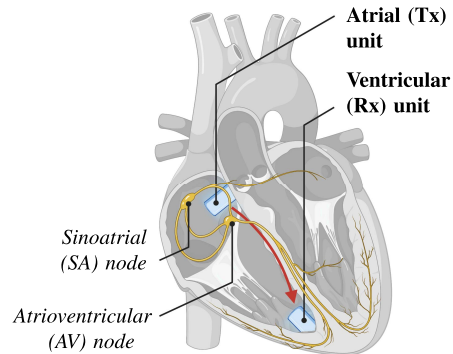


Fig. 1. Dual-chamber leadless pacemaker units located in the atria and right ventricle that communicate using the proposed PTM method.

In this letter, we propose a novel scheme for IBC in the heart which is inspired by biology and mimics well-studied communication between neurons. Namely, neural communication, referred to as temporal coding, relies on the precise timing of action potentials (spikes) or inter-spike intervals. Every spike train can be characterized by a discrete-time series. The series is then transmitted down the axon to the target cells, and it is this series that contains most, if not all, the information that the cell is conveying [7]. Cardiac action potentials (APs) differ considerably from neural APs. In a typical nerve, the AP duration is about 1 millisecond (ms). In contrast, the duration of cardiac APs ranges from 200 to 400 ms. Moreover, cardiac APs are generated solely for the purpose of pacing while neural APs are fired for the purpose of information communication. Since neural APs result either from spontaneous or stimulus-evoked activity, here we envision a scenario where cardiac APs similarly result either from spontaneous (sinoatrial node) or stimulus-evoked (pacemaker) activity. In this way, the pacemaker node located in the sinoatrial (SA) node can intervene in the pacing times, thus potentially modulating information onto the modified heartbeat sequence. A pacemaker node can sense the heartbeats as one of its basic tasks [8]. The modulated information should be detectable at any other node receiving the paces, as shown in Fig. 1. This unilateral communication method forms an information-theoretical broadcast channel [9]. We refer to it as the pace time modulation (PTM) method, which is structurally a type of pulse position modulation (PPM).

By embedding communication into pacing, PTM avoids using additional energy sources and devices (e.g. antennas, transceivers, leads, etc.) for communication, making it an attractive candidate for communication in multi-nodal pacemakers. Due to its simplicity and ease of implementation, PTM can play an important role, especially in scenarios wherein sensory and maintenance information needs to be

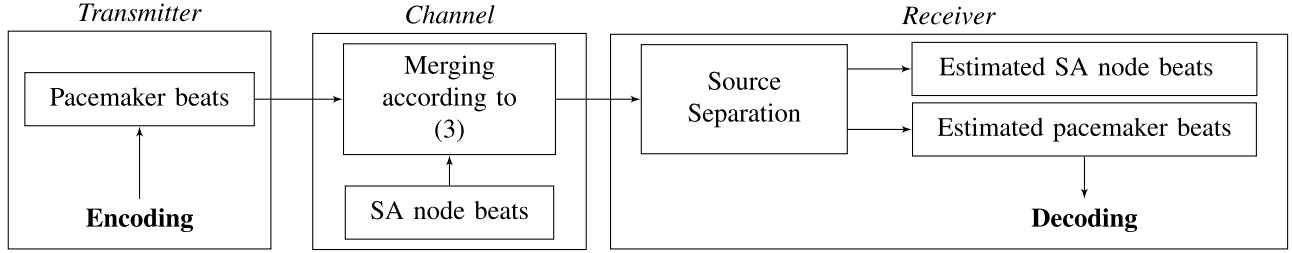


Fig. 2. Schematic representation of the system model. A merged sequence consisting of the transmitter and the SA node beats is received by the receiver. The uncertainty in the channel arises from the randomness of the SA node beats.

communicated from the main node to the other nodes of a multi-nodal pacemaker located at different pacing sites. The heart is innervated by vagal and sympathetic fibers which carry neural information from the medulla for sympathetic (increasing the heart rate) or parasympathetic (decreasing the heart rate) stimulation of the heart. The multi-nodal pacemaker can use PTM to communicate this information to the neighboring nodes in order to alter the pulsing in response to physiological demand [6]. Moreover, it can use PTM for communicating battery state information for its self-maintenance. However, PTM requires well-functioning atrioventricular conduction, as its main limitation.

## II. SYSTEM MODEL

In this section, we present the channel between two pacemaker nodes. First, a time-series modeling of the heartbeat sequence is given [10], and the channel is mathematically and illustratively presented. Subsequently, a discussion about source separation at the receiver is presented. The model represents the intrinsic heartbeat sequence as a point process. The occurrence of a contraction at time  $t_i$  is represented by an impulse  $\delta(t - t_i)$ , with  $\delta$  being the Dirac delta function. Under the assumption of no dispersion, the sequence of heartbeats is then represented by

$$h(t) = \sum_i \delta(t - t_i). \quad (1)$$

The point process of heartbeats is modeled as a fixed-dead-time-modified Poisson point process, which differs from a homogeneous Poisson process by the imposition of a dead-time interval after the occurrence of each event, during which the occurrence of new events is banned. This dead-time corresponds to the refractory period. The interevent-interval probability density function for the fixed-dead-time-modified Poisson point process of heartbeats assumes the exponential form [10]

$$f(t) = \begin{cases} 0 & t < \tau_d \\ \lambda e^{-\lambda(t-\tau_d)} & t \geq \tau_d, \end{cases} \quad (2)$$

where  $\tau_d$  is the dead-time and  $\lambda$  is the rate of the process before dead-time is imposed.

In the absence of the pacemaker, the SA node generates a sequence of heartbeats which is represented by (1). After the introduction of the pacemaker, the system will consist of two sources (the SA node and the pacemaker) contributing to the sequence of heartbeats. Each heartbeat can be initiated either by the SA node or the pacemaker, depending on whichever

trigger comes first. In other words, in every pacing interval, if the pacemaker triggers the heart before the SA node, the impulse from the SA node does not act, and vice versa. We can define the time of the  $n^{\text{th}}$  heartbeat as

$$t_n = \begin{cases} t_{Pn} & \text{if } t_{Pn} \leq t_{Sn} \\ t_{Sn} & \text{if } t_{Pn} > t_{Sn}, \end{cases} \quad (3)$$

where  $t_{Pn}$  and  $t_{Sn}$  are the triggering times from the pacemaker and the SA node, respectively. A schematic representation of the system model for PTM is given in Fig. 2. Here, we describe the three elements of the system model, namely the transmitter, the channel, and the receiver.

- **Transmitter:** The transmitter is the main pacemaker node. It encodes the information in the timings of the pacemaker beats.
- **Channel:** The two sequences of beats from the pacemaker and the SA node are merged by the channel according to (4). The triggering time of every beat that the pacemaker generates needs to be smaller than the corresponding time from the SA node to pass the channel.
- **Receiver:** The receiver pacemaker node receives the merged sequence of heartbeats and extracts the pacemaker beats sequence prior to decoding the information. Therefore, it needs to use a source separation method.

### A. Knowledge of $t_n$ at the Receiver

In this letter, we assume perfect synchronization between the transmitter and the receiver, i.e. we assume the times  $t_n$  to be perfectly detectable at the receiver. However, it is worth mentioning that at the implementation level, the effects of dispersion in the channel need to be taken into account. A comprehensive study on dispersion in Hodgkin-Huxley environments, which includes cardiovascular and neural media, as well as a method to equalize the dispersion effects when performing temporal coding is given in [11].

### B. Biocompatibility

By embedding communication into pacing, PTM requires neither any additional devices nor any additional types of signals (such as electromagnetic, acoustic, molecular, etc.) for its functioning, making it a less invasive communication concept compared to other methods. Moreover, PTM is highly flexible in terms of modulation symbols and block length which makes it easy to adjust it to various biological conditions. Lastly, PTM introduces variation in heartbeat intervals which has been recommended for pacemakers as it improves cardiac function [12].

### III. SOURCE SEPARATION AT THE RECEIVER

An uncertainty arises in this channel based on the fact that the receiver, on the basis of measurement of  $t_n$ , decides whether  $t_n = t_{Pn}$  or  $t_n = t_{Sn}$ , i.e. which of the cases in (3) has been realized. This arises the need for a source separation method at the receiver which we treat here as an inference problem. This is possible when prior information about the sources is available [13]. We assume the probability distributions of both the SA node- and pacemaker beats to be known. Then, a Bayesian approach can be used, and the problem simplifies down to a binary hypotheses test. We represent the hypotheses  $t_n = t_{Pn}$  and  $t_n = t_{Sn}$  by  $H = H_0$  and  $H = H_1$ , respectively. The binary hypothesis testing task is to optimally choose between the two hypotheses. Suppose  $H$  is modeled as a random quantity and assume that we know the *a priori* probabilities

$$\begin{aligned} P\{(H_0 \text{ is true})\} &= P(H = H_0) = P(H_0) = p_0, \\ P\{(H_1 \text{ is true})\} &= P(H = H_1) = P(H_1) = p_1. \end{aligned} \quad (4)$$

We model the quantity  $t_n$  at the receiver as the observation of a random variable  $T_n$ . We require the conditional densities  $f_{T_n|H_0}(t_n|H_0)$  and  $f_{T_n|H_1}(t_n|H_1)$  that tell us how  $t_n$  is distributed over the two hypotheses. They will be a part of the model that specifies how the measured data relates to the two hypotheses. According to (3), these conditional densities are

$$lf_{T_n|H}(t_n|H_0) = f_{t_{Pn}}(t_n), \quad f_{T_n|H}(t_n|H_1) = f_{t_{Sn}}(t_n). \quad (5)$$

#### Deciding With Minimum Conditional Probability of Error

In the absence of any measurement of  $T_n$ , a decision between  $H_0$  and  $H_1$  would have the following detection error events:

- With the choice  $H_0$ , we make a detection error when  $H_0$  does not hold. So, the probability of detection error, in this case, would be  $1 - P(H_0) = 1 - p_0$ .
- With the choice  $H_1$ , we make a detection error when  $H_1$  does not hold. So, the probability of detection error, in this case, would be  $1 - P(H_1) = 1 - p_1$ .

Thus, for the minimum probability of detection error, one should decide in favor of whichever hypothesis has maximum probability. The same reasoning applies when the objective is to decide between the two hypotheses with minimum probability of detection error, knowing the measurement  $T_n = t_n$ . In this case, we need to decide in favor of whichever hypothesis leads to minimum conditional probability  $P(\text{error}|T_n = t_n)$ . Thus, if  $P(H_1|T_n = t_n) > P(H_0|T_n = t_n)$ , we decide in favor of  $H_1$ , and if  $P(H_1|T_n = t_n) < P(H_0|T_n = t_n)$ , we decide in favor of  $H_0$ . This decision rule can be compactly written as

$$P(H_1|T_n = t_n) \stackrel{H_1}{\geq} P(H_0|T_n = t_n). \quad (6)$$

The corresponding probability of detection error is

$$\begin{aligned} &P(\text{error}|T_n = t_n) = \\ &\min\{1 - P(H_0|T_n = t_n), 1 - P(H_1|T_n = t_n)\}. \end{aligned} \quad (7)$$

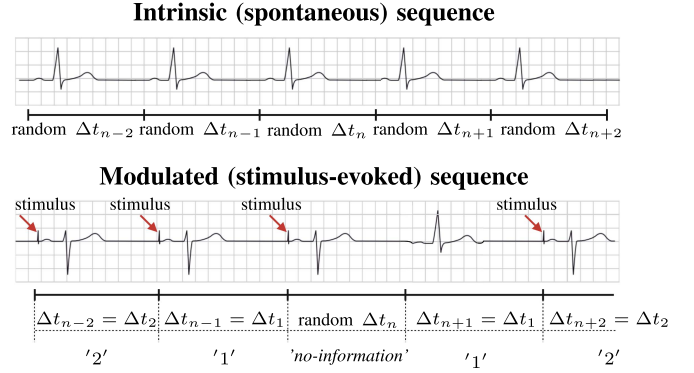


Fig. 3. Upper ECG sequence: intrinsic (spontaneous) sequence with  $\Delta t_i = \text{random } \Delta t_0$  that encodes *no information*. Lower ECG sequence: modulated (stimulus-evoked) sequence that encodes the data sequence “2–1–no information–1–2”.

### IV. PRACTICAL SCHEME

In this section, we present a practical scheme in which there is no need for the transmitter (pacemaker) to always intervene in pacing times, i.e. the transmitter can broadcast information on demand. Without loss of generality, the scheme is presented for the normal case where the average heart rate is 0.8 seconds (75 beats per minute). In this scheme, the pacemaker uses two symbols for its signaling, which are realized in two different pacing time differences. Moreover, a third case should be added which accounts for the case where the pacemaker does not transmit any information and therefore does not intervene in pacing. We refer to this case as the *no-information case*. The complete form of the communication scheme can therefore be written as

$$\begin{cases} \Delta t_n = 0.75 & \text{if } M_n = 1, \\ \Delta t_n = 0.76 & \text{if } M_n = 2, \\ \Delta t_n \text{ random} & \text{if } M_n = 0. \end{cases} \quad (8)$$

where  $M_n$  is the encoded symbol at timeslot  $n$ , and the time differences are given in seconds. We assign the symbol  $M_n = 0$  to the no-information case. For practical reasons, the two time differences used here for signaling are made slightly shorter than the average heartbeat rate (0.8 s). This considerably reduces the chance of a stimulus-evoked information signal coinciding with a spontaneous heartbeat. An illustration of this scheme is given in Fig. 3.

Based on the input data, the transmitter chooses the corresponding  $\Delta t_n$  and generates its trigger at  $t_{pn} = t_{n-1} + \Delta t_n$ . Finally, (3) is utilized to decide which of  $t_{Pn}$  or  $t_{Sn}$  gets realized.

#### A. MAP Decision Rule at the Receiver

In this part, we determine the *maximum a posteriori* (MAP) rule for the receiver to decide on the received symbol  $M_n \in \{0, 1, 2\}$  based on the measurement  $T_n = t_n$ . As both  $M_n = 1$  and  $M_n = 2$  fall into  $H_0$ , we define the two subhypotheses  $H_{01}$  and  $H_{02}$  to account for  $M_n = 1$  and  $M_n = 2$ , respectively. We implement the preceding MAP rule by utilizing Bayes' rule to express  $P(H_i|T_n = t_n)$  as

$$\frac{P(H = H_i)P(T_n = t_n|H = H_i)}{P(T_n = t_n)} \quad i = 01, 02, 1,$$

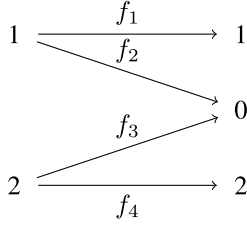


Fig. 4. Binary erasure channel structure corresponding to (8).

TABLE I  
JOINT PROBABILITY DISTRIBUTION  $p(X, Y)$

X \ Y	1	0	2
1	$0.6065p_{X1}$	$0.3935p_{X1}$	0
2	0	$0.3995p_{X2}$	$0.6005p_{X2}$

where the denominator can be dropped in the comparison as it functions as a scale factor.

For the MAP rule, we determine the three conditional probabilities of the abovementioned hypotheses given  $T_n = t_n$  and choose the hypothesis that corresponds to the maximum conditional probability. For instance, if  $P(H_{01}|T_n = t_n)$  is greater than  $P(H_{02}|T_n = t_n)$  and  $P(H_1|T_n = t_n)$ , the optimal decision for  $T_n = t_n$  is  $H_0$  or equivalently  $M_n = 1$ . This strategy is the extension of (6) for the ternary hypotheses. For this problem, it suffices to limit the comparison to three measurement cases:  $\Delta t_n = 0.75$ ,  $\Delta t_n = 0.76$ , and  $\Delta t_n$  random. Considering the fact that the channel model in Fig. 2 does not have noise but only erasures, and the fact that the probability of any continuous distribution taking on any specific value is zero, it is easy to recognize that the abovementioned conditional probabilities are maximized by the following decision rule:

$$\begin{cases} \text{If } \Delta t_n = 0.75 & \text{decide } M_n = 1, \\ \text{If } \Delta t_n = 0.76 & \text{decide } M_n = 2, \\ \text{If } \Delta t_n \text{ random} & \text{decide } M_n = 0. \end{cases} \quad (9)$$

### B. Achievable Rate

In contrast to typical communication schemes, the achievable rate of our proposed scheme is also a function of how often the pacemaker node needs to transmit information since the pacemaker in this scheme transmits information only on demand. Therefore, we derive the maximum achievable rate which corresponds to the case where the pacemaker transmits information at all time slots, i.e  $p_0 = 1$ , to get a better evaluation of its rate performance. The communication channel is illustrated in Fig. 4.

The probabilities  $f_1$ - $f_4$  are as follows:

$$\begin{aligned} f_1 &= P(t_{S_n} > 0.75) = 1 - \int_{-\infty}^{0.75} f(x)dx = 0.6065, \\ f_2 &= 1 - f_1 = 0.3935, \\ f_3 &= P(t_{S_n} < 0.76) = \int_{-\infty}^{0.76} f(x)dx = 0.3995, \\ f_4 &= 1 - f_3 = 0.6005, \end{aligned} \quad (10)$$

where  $f(\cdot)$  is given in (2). It can be seen that the channel has a nonsymmetric binary erasure channel (BEC) structure [9].

The marginal distribution of  $X$  is  $(p_{X1}, p_{X2})$  and the marginal distribution of  $Y$  is  $(0.6065p_{X1}, 0.3935p_{X1} + 0.3995p_{X2}, 0.6005p_{X2})$ . The maximum achievable rate of the communication scheme can now be written as

$$\begin{aligned} I(X; Y) &= H(X) + H(Y) - H(X, Y) \\ &= H(p_{X1}, p_{X2}) \\ &\quad + H(0.6065p_{X1}, 0.3935p_{X1} + 0.3995p_{X2}, 0.6005p_{X2}) \\ &\quad - H(0.6065p_{X1}, 0.3935p_{X1}, 0.3995p_{X2}, 0.6005p_{X2}). \end{aligned} \quad (11)$$

### C. Channel Coding

As it can be seen in TABLE I, the erasure probability of the communication channel in Fig. 4 is considerably high. In order to overcome this, we add channel coding to the communication scheme represented in (8). Since in this scheme the pacemaker does not transmit information at all time slots, the coding scheme needs to also take into account the time slots wherein the pacemaker is silent (no-information case) or namely the 0s. Therefore, the channel coding scheme should have the input alphabet  $\mathcal{X} = \{0, 1, 2\}$  and be ternary. We use the ternary (11,6,5)-Golay code [14] to obtain the numerical results to see how channel coding affects the performance of this communication scheme.

## V. NUMERICAL RESULTS

In this section, we give a numerical representation of the symbol error rates (SERs) and achievable rates of the coded and uncoded PTM schemes that we introduced in Section IV. The exponential distribution presented in (2) is a good candidate for theoretical analysis and deriving theoretical bounds. However, it is not a suitable candidate for generating realistic heartbeat sequences due to its very high and unrealistic variance. There exist several models for generating realistic heartbeat sequences [10], amongst which we use the fractal-Gaussian-noise driven integrate-and-fire model, showing considerable agreement with real data. In the model, a fractal-Gaussian-noise is used as the kernel of an integrate-and-fire model, generating the beats. The results are generated in MATLAB.

To clarify, a 20000-symbol sequence is generated and then mapped to the corresponding time intervals  $\Delta t_n$  based on (8). The first heartbeat is generated by the SA node. Afterwards, for each time slot  $n$ ,  $t_{P_n} = t_{n-1} + \Delta t_n$  is compared with  $t_{S_n}$  generated by the integrate-and-fire model, and  $t_n$  is decided by (3). At the receiver, the MAP rule given in (9) is utilized to detect the symbols since it is valid for every continuous distribution for  $t_{S_n}$ . In the channel-coded case, the symbol sequence is first encoded and thereafter mapped to time intervals  $\Delta t_n$ . At the receiver, the symbols are detected one by one but decoded blockwise. A combined detection and

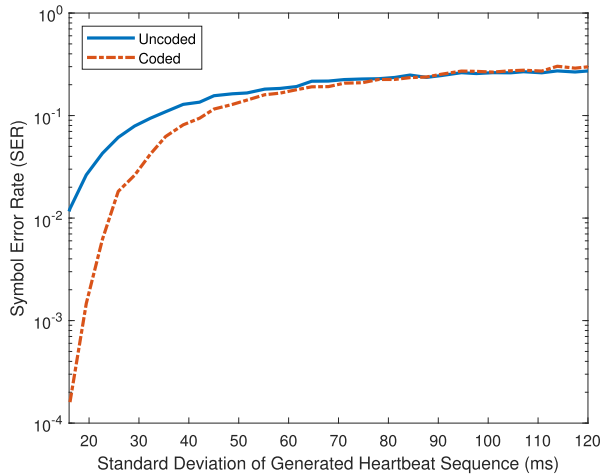


Fig. 5. Average SERs of the coded and uncoded PTM schemes vs. the standard deviation of the generated heartbeat sequences for the realistic heartbeat model.

decoding method is not of interest in this work because of its complexity.

In Fig. 5, the symbol error rates of the coded and uncoded schemes are compared. We have increased the standard deviation of the kernel noise of the integrate-and-fire model, which results in an increase in the standard deviation of the inter-beat intervals ( $\Delta t_{S_n}$ ) in the generated heartbeat sequences. The symbol error rates are plotted vs. the resulting standard deviation of the generated heartbeat sequences, on a logarithmic scale. As it can be seen, the coded scheme performs considerably better than the uncoded scheme in the *low-noise* regime, but the difference in performance narrows with the increase in noise level. A variation of more than 120 ms in the heartbeats is considered abnormal [15]. Therefore, the simulation results are plotted up to this natural constraint.

Recall that Fig. 5 is obtained for the aforementioned fractal-Gaussian-noise driven integrate-and-fire model. We have also run similar simulations to obtain analogous results for the exponential distribution presented in (2). It appears that the symbol error rates for the case of exponential distribution are considerably higher than the ones for the integrate-and-fire model, which is mainly due to its very high standard deviation. The standard deviation of an exponential distribution with a mean of 0.8 s is 800 ms (equal to the mean), which is more than six times larger than the stopping point of 120 ms in Fig. 5. In other words, an exponential distribution provides a worst-case scenario and therefore should only be used for computing capacity and upper bounds on the probability of error, since it has the highest entropy among all non-negative random variable distributions which have the same mean value [9]. It is also worth mentioning that in this work we have followed the same line as in [10], where the theory is based on the fixed-deadtime-modified Poisson point process, but heartbeat sequences are generated with different models due to the mentioned reasons.

N.B. As stated in the abstract, this communication scheme does not deviate the heart rate from its normal range. There are two arguments to support this statement. First, the marginal

probability of  $Y = 0$  in TABLE I is considerably high which means that the natural heartbeats will be realized for a considerable proportion of the time. Second, the deviation which can be caused by the modulation scheme in (8) is obviously less than 0.05 s, which is less than the natural constraint of 0.12 s [15].

## VI. CONCLUSION

In this letter, the PTM scheme for communication in cardiac was introduced, analyzed, and tested through an illustrative achievable rate scheme. The presented analysis and achievable rate schemes assume the average heart rate to be constant at all timeslots. Since the average heart rate is realistically not constant and changes due to activity or for considerably many pathological reasons, future work on this concept should consider adaptive communication schemes, which can switch between different constellations according to the changes of the average heart rate.

## REFERENCES

- [1] M. Ghamari, B. Janko, R. S. Sherratt, W. Harwin, R. Piechockic, and C. Soltanpur, "A survey on wireless body area networks for healthcare systems in residential environments," *Sensors*, vol. 16, no. 6, p. 831, 2016.
- [2] W. J. Tomlinson, S. Banou, C. Yu, M. Stojanovic, and K. R. Chowdhury, "Comprehensive survey of galvanic coupling and alternative intra-body communication technologies," *IEEE Commun. Surveys Tuts.*, vol. 21, no. 2, pp. 1145–1164, 2nd Quart., 2019.
- [3] N. B. Asan, "Fat-IBC: A new paradigm for intra-body communication," Ph.D. thesis, Fac. Sci. Technol., Acta Universitatis Upsaliensis, Uppsala, Sweden, 2019.
- [4] T. Nakano, M. Moore, A. Enomoto, and T. Suda, "Molecular communication technology as a biological ICT," in *Biological Functions for Information and Communication Technologies*. Berlin, Germany: Springer, 2011, pp. 49–86.
- [5] N. Tokavanich *et al.*, "A network meta-analysis and systematic review of change in QRS duration after left bundle branch pacing, his bundle pacing, biventricular pacing, or right ventricular pacing in patients requiring permanent pacemaker," *Sci. Rep.*, vol. 11, no. 1, pp. 1–8, Dec. 2021.
- [6] R. G. Trohman, H. D. Huang, T. Larsen, K. Krishnan, and P. S. Sharma, "Sensors for rate-adaptive pacing: How they work, strengths, and limitations," *J. Cardiovascular Electrophysiol.*, vol. 31, no. 11, pp. 3009–3027, Nov. 2020.
- [7] F. Gabbiani and C. Koch, "Principles of spike train analysis," *Methods Neuronal Model.*, vol. 12, no. 4, pp. 313–360, 1998.
- [8] S. S. Barold and J. J. Gaidula, "Evaluation of normal and abnormal sensing functions of demand pacemakers," *Amer. J. Cardiol.*, vol. 28, no. 2, pp. 201–210, Aug. 1971.
- [9] T. M. Cover and J. A. Thomas, *Elements of Information Theory*. Hoboken, NJ, USA: Wiley, 2006.
- [10] M. C. Teich, S. B. Lowen, B. M. Jost, K. Vibe-Rheymer, and C. Heneghan, "Heart rate variability: Measures and models," in *Nonlinear Biomedical Signal Processing*, vol. 2. New York, NY, USA: Wiley, 2001, pp. 159–213.
- [11] R. N. Miller and J. Rinzel, "The dependence of impulse propagation speed on firing frequency, dispersion, for the Hodgkin–Huxley model," *Biophys. J.*, vol. 34, no. 2, pp. 227–259, May 1981.
- [12] J. Shanks *et al.*, "Reverse re-modelling chronic heart failure by reinstating heart rate variability," *Basic Res. Cardiol.*, vol. 117, no. 1, pp. 1–16, Dec. 2022.
- [13] A. Mohammad-Djafari and K. Knuth, *Handbook of Blind Source Separation*. Oxford, U.K.: Academic, 2010, ch. 12, pp. 467–513.
- [14] M. J. Golay, "Notes on digital coding," *Proc. IEEE*, vol. 37, p. 657, Jun. 1949.
- [15] J. E. Olgin and D. P. Zipes, *Braunwald's Heart Disease: A Textbook of Cardiovascular Medicine*, 11th ed. Amsterdam, The Netherlands: Elsevier, 2018, ch. 40, pp. 772–779.